Journal of Biomolecular NMR, **19:** 19–31, 2001.
KLUWER/ESCOM

Sugar conformation of a stereospecific 2′-R or 2′-S deuterium-labeled DNA decamer studied with proton-proton J coupling constants

Chojiro Kojima[a,b], Etsuko Kawashima[c], Takeshi Sekine[c], Yoshiharu Ishido[c], Akira Ono[d], Masatsune Kainosho[b,d] & Yoshimasa Kyogoku[a,e,*]

[a]*Institute for Protein Research, Osaka University, Suita, Osaka 565-0871, Japan;* [b]*CREST (Core Research Evolutional Science and Technology), Japan Science and Technology Corporation (JST), Kawaguchi, Saitama 332-0012, Japan;* [c]*Laboratory of Pharmaceutical Chemistry, Faculty of Pharmacy, Tokyo University of Pharmacy and Life Science, Hachioji, Tokyo 192-0397, Japan;* [d]*Department of Chemistry, Faculty of Science, Tokyo Metropolitan University, Hachioji, Tokyo 192-0392, Japan;* [e]*Department of Applied Physics and Chemistry, Fukui Institute of Technology, Fukui, Fukui 910-8505, Japan*

Received 21 June 2000; Accepted 5 October 2000

Key words: DNA sugar conformation, Gaussian distribution model, harmonic motion, Karplus equation, proton-proton J coupling constant, stereospecific deuterium labeling, two-site jump model

Abstract

The sugar conformation of a DNA decamer was studied with proton-proton ^{3}J coupling constants. Two samples, one comprising stereospecifically labeled 2′-R-^{2}H for all residues and the other 2′-S-^{2}H, were prepared by the method of Kawashima et al. [*J. Org. Chem.* (1995) **60**, 6980–6986; *Nucleosides Nucleotides* (1995) **14**, 333–336], the deuterium labeling being highly stereospecific ($\geq$ 99% for all 2″-^{2}H, $\geq$ 98% for 2′-^{2}H of A, C, and T, and $\geq$ 93% for 2′-^{2}H of G). The ^{3}J values of all H1′-H2′ and H1′-H2″ pairs, and several H2′-H3′ and H2″-H3′ pairs were determined by line fitting of 1D spectra with 0.1–0.2 Hz precision. The observed J coupling constants were explained by the rigid sugar conformation model, and the sugar conformations were found to be between C3′-exo and C2′-endo with Φ_m values of 26° to 44°, except for the second and 3′ terminal residues C2 and C10. For the C2 and C10 residues, the lower fraction of S-type conformation was estimated from $J_{H1'H2'}$ and $J_{H1'H2''}$ values. For C10, the N–S two-site jump model or Gaussian distribution of the torsion angle model could explain the observed J values, and 68% S-type conformation or C1′-exo conformation with 27° distribution was obtained, respectively. The differences between these two motional models are discussed based on a simple simulation of J-coupling constants.

Introduction

The deoxyribose conformation is one of the most important parameters for describing a nucleic acid structure. It has been extensively studied and reported to be a single conformation or an equilibrium between the N-type (C3′-endo) and S-type (C2′-endo) conformations (Rinkel and Altona, 1987; Widmer and Wüthrich, 1987; Bax and Lerner, 1988; Salazar et al., 1993; Wijmenga et al., 1993; Schmitz and James, 1995; Conte et al., 1996). In such studies accurate and precise $^3J_{HH}$ values between the sugar protons are required. Spin simulation methods of 2D COSY such as SPHINX and LINSHA (Widmer and Wüthrich, 1986) or advanced heteronuclear techniques such as HCCH-E.COSY (e.g. Ono et al., 1994) can give us J coupling constants with relatively high precision ($\leq$ 0.5 Hz). More accurate and precise J coupling constants will be obtained when the stereospecific deuterium-labeling procedure is applied at the methylene sites (Huang et al., 1990; Wang et al., 1992; Kawashima et al., 1993, 1995a, b; Curley et al., 1994; Yang et al., 1997). With deuterium labeling at the methylene groups the

*To whom correspondence should be addressed. E-mail: kyogoku@protein.osaka-u.ac.jp

spin system is drastically simplified and the dipolar interference with the scalar interaction (Harbison, 1993; Zhu et al., 1994; Cavanagh et al., 1996) is attenuated, eliminating the strong dipolar interaction between the two methylene protons (1.75 Å). In this study, the sugar conformation of a DNA decamer, $d(GCATTAATGC)_2$, is studied using two deuterium-labeled samples, one comprising stereospecific 2′-R-^{2}H at all residues and the other 2′-S-^{2}H. The global conformation of this DNA oligomer is B-form-like, as determined by NMR (Chazin et al., 1986; Kojima et al., 1998a). The labeling efficiency of our procedure (Kawashima et al., 1993, 1995a, b; Yang et al., 1997) is higher and more stereospecific than the previous one (Huang et al., 1990; Wang et al., 1992; Foldesi et al., 1993; Yamakage et al., 1993; Agback et al., 1994).

Materials and methods

The 2′-R or 2′-S deuterium-labeled 2′-deoxy mononucleotide was prepared by the reported procedure (Kawashima et al., 1993, 1995a, b). The deuterium labeling efficiency was estimated to be $\geq$ 99% for all 2′-R-^{2}H, $\geq$ 98% for 2′-S-^{2}H of A, C, and T, and $\geq$ 93% for 2′-S-^{2}H of G on ^{1}H 1D NMR. The 3′-phosphoramidite of each nucleotide was used for oligonucleotide synthesis with a DNA synthesizer (Applied Biosystems Inc., ABI 392). The sequence was 5′-^{1}G^{2}C^{3}A^{4}T^{5}T^{6}A^{7}A^{8}T^{9}G^{10}C-3′, the residue numbers used in this report being shown. The details of the purification procedure were reported previously (Kyogoku et al., 1995). The NMR sample was dissolved in 400 μl of 20 mM phosphate buffer containing 50 mM NaCl, adjusted to pH 6.8, lyophilized and then dissolved in D_2O. The resulting solution was degassed and kept in a 5 mm tube. The double-strand concentration was estimated to be 3 mM from the UV absorbance.

The signal assignments were given previously (Chazin et al., 1986; Kojima et al., 1998a), and confirmed here by DQF-COSY experiments. The stereospecific assignments of the sugar H2′ and H2″ resonances were easily confirmed, with clear identification of the H2′ and H2″ resonances for C10 (overlapping). The DQF-COSY spectra were recorded with a Bruker ARX 500 spectrometer operating at a ^{1}H frequency of 500 MHz at 30 °C, with a spectral width of 4000 Hz for both dimensions, and 512 hyper complex points for t1 and 512 complex points for t2. A π/4 shifted sinebell window function was applied and zero-filled to 1024 real points for both dimensions. The pulse repetition delay time was 2 s and 128 scans were employed for each t1 increment. Phase-sensitive detection in t1 was performed by the TPPI-States method (Marion et al., 1989). The ^{31}P resonance was decoupled with a π pulse in t1 and WALTZ16 in t2.

The longitudinal relaxation time, T_1, of the H1′ resonance was determined by the inversion-recovery method. The pulse repetition delay time was 30 s and 11 inversion-recovery delay times were used: 0.23, 0.48, 0.76, 1.06, 1.40, 1.78, 2.23, 2.75, 3.40, 4.22, and 28.8 s. For each spectrum, 32 scans and 8K complex points per 4000 Hz were recorded, and zero-filled to 64K points. The peak intensities of the H1′ resonance in 11 spectra, together with the line widths and J coupling constants ($J_{H1'H2'}$ or $J_{H1'H2''}$), were obtained with the 1D fitting procedure of FELIX (Biosym Technologies), and used for the relaxation time determination with the equation $\text{Intensity} = I_0 * [1 - 2 * \exp(-t/T_1)]$, where I_0 and T_1 were optimized. 3–5 spectra with a good S/N ratio out of the 11 were used to measure the splitting of the well-separated H2′ or H2″ signals, $J_{H1'H2'}+J_{H2'H3'}$ or $J_{H1'H2''}+J_{H2''H3'}$, respectively. The average line width and J values were used for further calculation. The error on averaging was about 0.1 Hz for J values (less than 0.2 Hz), and 5% for the line width. The apparent transverse relaxation time, T_2^*, was related to the apparent line width, $1/T_2^* = \pi \times$ line width. The overall rotational correlation time, τ_o, was determined minimizing the difference between the observed and calculated T_1/T_2 ratios, with the equations $T_1/T_2 = (3J(0) + 5J(\omega) + 2J(2\omega))/(2J(\omega) + 8J(2\omega))$, and $J(n\omega) = \tau_o/(1+n^2\omega^2\tau_o^2)$, where ω is the ^{1}H resonance frequency ($2\pi \times 500 \times 10^6$ rad/s) (Abragam, 1961). The vicinal proton-proton J-coupling constants were related to the DNA sugar conformation with the generalized Karplus equation optimized for β-D-deoxyribose (Haasnoot et al., 1980; Wijmenga et al., 1993). For most of the calculations Microsoft Excel 98 (Microsoft) was used with the Solver Add-in function and Visual Basic-based macro programs.

Results

Effects of deuterium labeling

Three DQF-COSY spectra for the non-labeled, 2′-R deuterium-labeled (2′-^{1}H, 2″-^{2}H) and 2′-S deuterium-labeled (2′-^{2}H, 2″-^{1}H) decamers are shown in Figure 1a, b and c, respectively. The cross peaks between

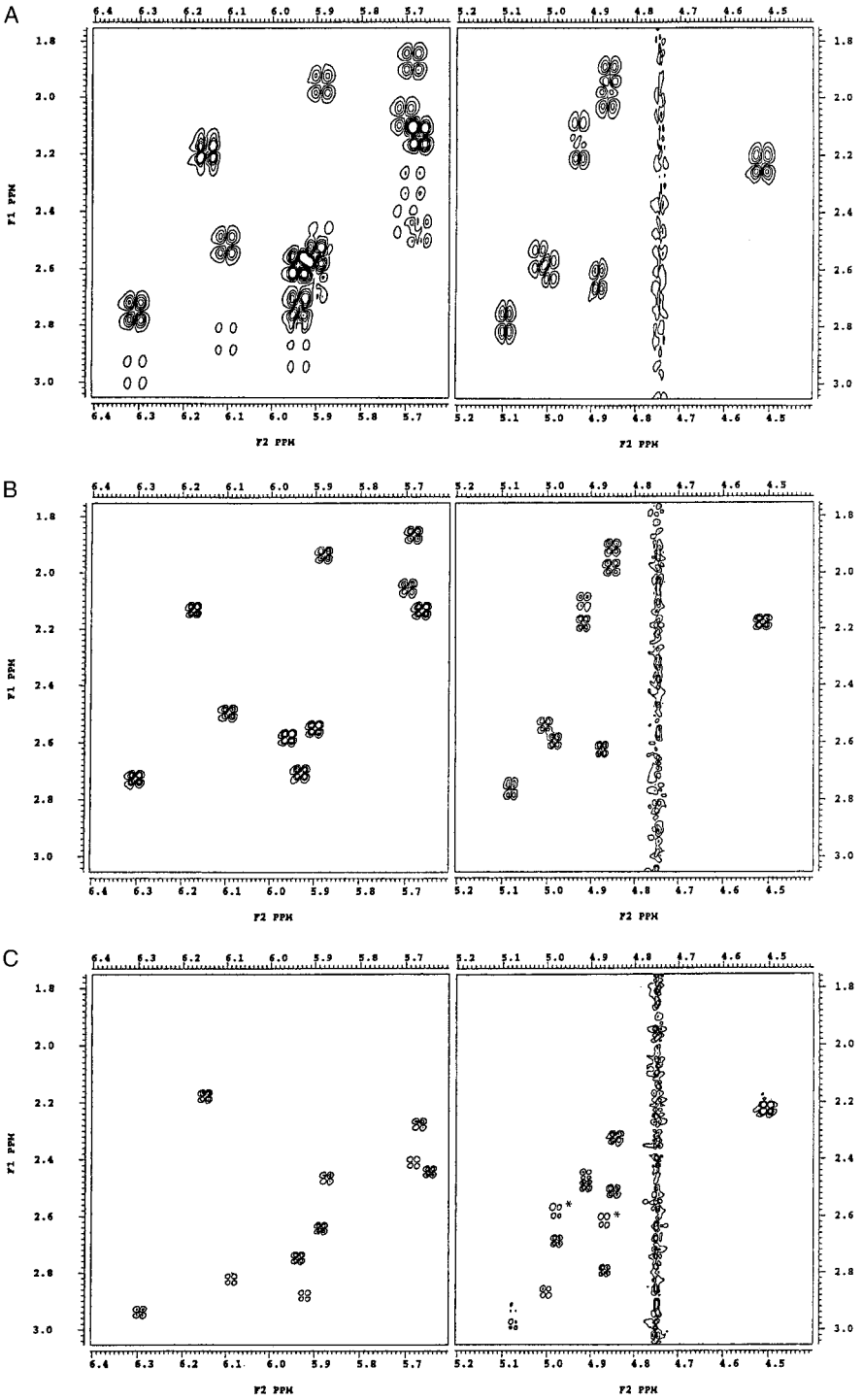

Figure 1. Two-dimensional DQF-COSY spectra of the (A) non-labeled, (B) 2′-R ^{2}H (2′-^{1}H, 2″-^{2}H)-labeled, and (C) 2′-S ^{2}H (2′-^{2}H, 2″-^{1}H)-labeled DNA decamer. The spectra were recorded with a Bruker ARX 500 spectrometer at 30 °C with 512 hypercomplex points for t1 and 512 complex points for t2, multiplying the π / 4 shifted sinebell window function for both dimensions, and zerofilled to 1024 real points for both dimensions. The pulse repetition delay time was 2 s. The phase sensitive detection for t1 was performed by the TPPI-States method. The ^{31}P resonance was decoupled by a π pulse for t1 and WALTZ16 for t2, but the ^{2}H one was not. The sample solution contained 3 mM duplex with 20 mM phosphate buffer and 50 mM NaCl, pH 6.8. The base sequence was 5′-GCATTAATGC-3′. The left panel in each figure shows the cross peaks between the H1′ (F2) and H2′/H2″ (F1) resonances, and the right one those between H3′ (F2) and H2′/H2″ (F1).

Table 1. T_1 and T_2^* values of the H1′ resonance and the overall correlation time τ_o for the 2″- or 2′-deuterium-labeled DNA decamer at 30 °C[a]

	G1	C2	A3	T4	T5	A6	A7	T8	G9	C10
T_1 (s)										
2″-^{2}H[b]	2.95	3.34	3.01	3.36	3.20	3.03	2.95	3.12	3.04	3.71
2′-^{2}H	2.84	2.95	3.07	3.11	3.11	2.89	3.05	3.00	2.99	3.33
T_2^* (s)										
2″-^{2}H	0.114	0.089	0.084	0.081	0.081	0.067	0.064	0.072	0.102	0.121
2′-^{2}H	0.068	0.072	0.065	0.069	0.057	0.053	0.052	0.059	0.066	0.087
τ_o (ns)										
2″-^{2}H	1.8	2.2	2.1	2.3	2.3	2.4	2.4	2.4	2.0	2.0
2′-^{2}H	2.3	2.3	2.5	2.4	2.7	2.7	2.8	2.6	2.4	2.2

[a]The non-selective inversion-recovery method and the apparent linewidth ($1/T_2^* = \pi *$ half-height full-linewidth) were used for T_1 and T_2^* determination, respectively. The overall correlation time was obtained by minimizing the difference between each simulated T_1/T_2 and observed T_1/T_2^* ratio. Assuming simple isotropic tumbling, the T_1/T_2 values were evaluated as follows, $T_1/T_2 = (3J(0) + 5J(\omega) + 2J(2\omega)) / (2J(\omega) + 8J(2\omega))$, where $J(n\omega) = \tau_o / (1 + n^2\omega^2\tau_o^2)$, and ω is the spectrometer frequency in rad/s. The averaged correlation times were 2.3, 2.2, and 2.5 ns for all sets, and the 2″-^{2}H, and 2′-^{2}H data sets, respectively.

[b]2″-^{2}H is the data set for the stereospecifically deuterium-labeled oligomer, which has the 2′-R deuterium (2′-^{1}H, 2″-^{2}H) stereochemical configuration, and on the contrary, 2′-^{2}H is that for (2′-^{2}H, 2″-^{1}H).

the H2′/H2″ resonance (ω1) and H1′ (ω2, left) or H3′ (ω2, right) are shown. In these three spectra the recording and processing parameters were identical. Small chemical shift differences were observed among the three spectra. Most of the differences were up-field shifts upon deuteration in the sugar ring, and thus these phenomena can be explained by the secondary isotope shift. Additionally, slight differences in the solution conditions may contribute to the small changes in the chemical shifts. The spin system was simplified and the apparent line width was remarkably reduced because of the lack of dipolar and scalar interactions between the methylene protons. In fact, the longitudinal relaxation times estimated by null point analyses were lengthened about 1.5 times for the 1′ proton (data not shown). The COSY cross peaks between H2″ and H3′ can be clearly seen in Figure 1c (deuterium-labeled), but not in Figure 1a (non-deuterium labeled) because of the broader line width of H2″ and the complex J-splitting pattern of the non-labeled sample. Similar phenomena were seen for the H1′-H2″ cross peaks. H2′-H3′ cross peaks of the guanosine residue, indicated by the asterisk in Figure 1c, were seen, which should not be detected, i.e., the H2′ (= 2′-pro-S) proton was replaced by deuteron in this sample. This was not due to the sugar conformation of the guanosine residues, because it was not different from the others (Chazin et al., 1986). The cross peaks can be explained in two ways; first, the efficiency of the deuterium labeling for the guanosine residues (≥ 93%) was lower than for the others (≥ 98%), and second the J-coupling constants of H2′-H3′ (∼6 Hz) were larger than those of H2″-H3′ (∼1 Hz). For the 2′-S deuterium-labeled sample, however, no cross peak was found between H1′ and H2′, and the splitting pattern of most cross peaks in the COSY spectrum was quite simple even for the guanosine residues. Thus the efficiency of our deuterium labeling was sufficient to study the J coupling constants for the 2′-R deuterium-labeled (2′-^{1}H, 2″-^{2}H) sample and the 2′-S deuterium-labeled (2′-^{2}H, 2″-^{1}H) A, C, and T. The 2′-S deuterium-labeled G may have small systematic errors in the apparent J coupling constants, since the suppression of the H2′-H3′ cross peaks in the COSY spectrum was not perfect.

The longitudinal relaxation time, T_1, and the apparent transverse relaxation time, T_2^*, of the H1′ resonance are shown in Table 1 for both the 2′-R and 2′-S deuterium-labeled samples. There are no big differences in T_1 between these two samples (≤ 10%) or among the whole residues (≤ 20%). For T_2^* differences are clear between the two samples (20–40%) and among all residues (40–50%). The longest T_1 and T_2^* were found for the 3′ terminal residue. Since the intra-residue H1′-H2″ distance (2.2 Å) is shorter than that of H1′-H2′ (2.8 Å) for the canonical B-DNA conformation, both T_1 and T_2^* of the 2′-R deuterium-labeled sample (2′-^{1}H, 2″-^{2}H) are expected to be longer than those of 2′-S. Actually, this is true

Table 2. Observed J coupling constants for the 2″- or 2′-deuterium-labeled DNA decamer and determined sugar conformation[a]

	G1	C2	A3	T4	T5	A6	A7	T8	G9	C10
Observed data										
$J_{H1'H2'}$	9.1	9.4	9.4	9.1	9.4	9.8	8.9	8.6	9.5	7.3
$J_{H1'H2'} + J_{H2'H3'}$	14.7	#	#	16.8	16.4	#	15.7	16.3	15.4	#
$J_{H1'H2''}$	6.3	5.2	5.4	6.3	6.0	6.0	5.5	6.3	5.7	6.9
$J_{H1'H2''} + J_{H2''H3'}$	##	##	##	##	##	##	##	##	##	10.7
Sugar	C3′	C3′	C3′	C2′	C2′	C2′	C2′	C2′	C2′	–
conformation	-exo	-exo	-exo	-endo	-endo	-endo	-endo	-endo	-endo	
P (deg)	186.2	201.8	194.1	147.5	156.5	154.8	173.8	165.3	173.6	–
Φ_m (deg)	33.0	52.1	43.6	28.1	30.6	32	32.3	26.3	33.9	–
RMSD	0.2	0.0	0.0	0.2	0.2	0.0	0.5	0.4	0.1	≥0.7
%S	95	83	86	95	95	102	79	87	92	76

[a]J values (in Hz) determined by the fitting of 1D spectra. $J_{H1'H2'}$ and $J_{H1'H2'} + J_{H2'H3'}$ (or $J_{H1'H2''}$ and $J_{H1'H2''} + J_{H2''H3'}$) values were derived from the splitting of the H1′ and H2′ (or H2″) resonances of the 2″- (or 2′-) deuterium-labeled oligomer, respectively.
#: Not determined due to overlap.
##: Not determined qualitatively, but each $J_{H2''H3'}$ was estimated to be less than 2.5 Hz based on the splitting pattern and the line width of the H2″ signals.
The sugar conformation was characterized by two parameters of the phase angle of pseudorotation, P, and the pucker amplitude, Φ_m, where each parameter was optimized by minimizing the RMSD between observed and simulated J coupling constants. For the C10 residue the sugar conformation was not determined uniquely. The approximate fraction of S-type conformer (%S) was determined by the equation: %S = (Σ1′ − 9.4) / (15.7 − 9.4) (van Wijk et al., 1992).

except for T_1 of A3 and A7. The three-dimensional coordinates of this molecule are not available so far, but once available, a complete relaxation matrix calculation (e.g. CORMA (Keepers and James, 1984)) would explain the difference between them more clearly. Assuming the apparent T_2^* as a real T_2, the ratio of T_1 to T_2^* is related to the overall correlation time for each residue. When the proton-proton dipolar interaction is a dominant relaxation mechanism for the H1′ proton, $T_1/T_2 = (3J(0) + 5J(\omega) + 2J(2\omega))/(2J(\omega) + 8J(2\omega))$, where ω = a spectrometer frequency, and $J(n\omega) = \tau_o / (1+n^2\omega^2\tau_o^2)$ for a rigid isotropic molecule. The calculated correlation time, τ_o, is in the range of 1.8 to 2.8 s, and the average value is 2.3 ns. The sequence dependent differences are below 0.6 ns for both the 2′-R and 2′-S deuterium-labeled samples. They exhibit a similar tendency, that is, the apparent overall correlation times of T5, A6, A7, and T8 are larger than those of the others. If the TAAT part (from T5 to T8) of our DNA has a more rigid structure than the others on the nanosecond time scale, the experimental variation in the correlation time depending on the sequence can be explained. However, this is one of the possible explanations, thus the details of the motion should be examined using other methods (see Lane, 1993; Kojima et al., 1998b). Another feature is that the correlation time of the 2′-R deuterium-labeled sample is always smaller than that of 2′-S. The difference is about 0.3 ns (0.1–0.5 ns) and thus relatively small (≤ 20%), but these systematic differences should not be neglected. The overall correlation time should be unique for both samples, thus the difference seemed to originate from the sample preparation and/or the correlation time estimation. However, the average correlation time of 2.3 ns agreed with the empirical value of $2 \sim 3$ ns estimated from the relation between the correlation time and the number of base pairs (Eimer et al., 1990; Lane, 1993).

Proton-proton J-coupling constants and sugar conformation

The proton-proton vicinal J-coupling constants ($^3J_{HH}$) determined by the 1D fitting procedure (vide supra) are shown in Table 2 for both the 2′-R and 2′-S deuterium-labeled samples. Two values, $J_{H1'H2'}$ and $J_{H1'H2'} + J_{H2'H3'}$, were obtained from the splitting of the H1′ and H2′ resonances of the 2′-R deuterium-labeled sample, and another two, $J_{H1'H2''}$ and $J_{H1'H2''} + J_{H2''H3'}$, from the splitting of the H1′ and H2″ resonances of the 2′-S deuterium-labeled sample, respectively. The long-range J-couplings were not considered. Each H1′ signal is a doublet, and the difference between the frequencies is assumed to be $J_{H1'H2'}$ or

$J_{H1'H2''}$. On the contrary, the splitting pattern of the H2′ or H2″ resonance is complex, i.e., a doublet, triplet or quartet. This depended on the line width and two J values, $J_{H1'H2'}$ and $J_{H2'H3'}$, for the 2′-R deuterium-labeled sample, and $J_{H1'H2''}$ and $J_{H2''H3'}$ for 2′-S. A doublet is observed when one of the J values is much smaller than the line width and the other is larger, and this is the case for the H2″ resonance except for that of the 3′ terminal residue C10, which is a triplet. A triplet is observed when the difference between the two J values is much smaller than the line width, and this is the case for the H2′ resonance. In both cases the sum of the J-coupling constants, $J_{H1'H2'} + J_{H2'H3'}$ or $J_{H1'H2''}+J_{H2''H3'}$, was determined from the frequency difference between the outer peaks of the H2′ or H2″ splitting, respectively. All $J_{H1'H2'}$ and $J_{H1'H2''}$ values, six of the ten $J_{H1'H2'} + J_{H2'H3'}$ values, and one $J_{H1'H2''} + J_{H2''H3'}$ value were determined quantitatively. Four $J_{H1'H2'} + J_{H2'H3'}$ values were not determined due to peak overlap. Nine $J_{H1'H2''} + J_{H2''H3'}$ values were not determined quantitatively, but the $J_{H2''H3'}$ values were semi-quantitatively assumed to be less than 2.5 Hz. This is because the H2″ resonance is a clear doublet and the observed $J_{H1'H2''}$ values, 5–7 Hz, were equal to or larger than the line width, 3–7 Hz. It should be noted that these J-coupling constants cannot be determined so easily and precisely without stereospecific deuterium-labeling.

These determined J-coupling constants were used for conformational analysis of deoxyribose. Using the Karplus equation (Haasnoot et al., 1980; Wijmenga et al., 1993) the pseudo-rotation angle P and pucker amplitude Φ_m were optimized by minimizing the root mean square differences, RMSD, of the observed and simulated J-coupling constants. As shown in Table 2, most residues except for C10 were judged to be acceptable based on the following two criteria: (1) RMSD is less than 0.7 Hz and (2) $J_{H2''H3'}$ is less than 2.5 Hz except for C10. The RMSD criterion of 0.7 Hz was determined from the sum of two errors, 0.1–0.2 Hz originating from the experiment and 0.48 Hz from the Karplus parameter. The Karplus parameter used here was previously determined by Altona and his collaborators, who optimized 315 proton-proton vicinal J-coupling constants, and the intrinsic error was obtained from the RMSD of the fitting, 0.48 Hz (Haasnoot et al., 1980). Thus the observed proton-proton vicinal J-coupling constants were explained by the rigid single conformation for most residues. The exception, the 3′ terminal residue C10, was carefully examined as shown later.

The determined pseudo-rotation angle P and pucker amplitude Φ_m were in the empirically acceptable ranges as S-type sugar conformation, where P $= 162° \pm 40°$ and $\Phi_m = 36.4° \pm 10°$. The Φ_m value of the C2 residue was exceptionally large. As seen in the cases of the C2 and A3 residues, the small difference in the observed J values caused the large differences in the determined conformational parameters (see Table 2). That is, even though the error of the observed J values was small (0.1–0.2 Hz), that of the determined conformational parameters could be relatively large ($\sim 10°$ for Φ_m). There was a possibility that the single conformation model was not appropriate for the C2 residue. The approximate fraction of S-type sugar conformation was calculated using a simple equation, %S = (S1′ − 9.4) / (15.7 − 9.4) (van Wijk et al., 1992), with observed $J_{H1'H2'}$ and $J_{H1'H2''}$. The results are given in Table 2, and the C2, A3, A7, T8, and C10 residues showed a lower fraction. Thus for the C2 residue, the lower fraction of S-type conformation may be more probable since its Φ_m value was exceptionally large.

Motional models and the sugar conformation of the 3′ terminal residue

The 2′-deoxyribose ring of the 3′ terminal residue could be flexible and the observed J values may have some contribution from local motion through time averaging. Here one rigid conformational model and two motional models were considered to take into account the motional averaging, (**A**) no fluctuation, (**B**) classical harmonic motion, and (**C**) two-site jump motion. The basic assumption for model (**A**) is the presence of a quite stable single conformation characterized by two parameters, the phase angle of pseudorotation, P, and the pucker amplitude, Φ_m. This model (**A**) was already used to determine the sugar conformation (vide supra). In model (**B**) the classical harmonic motion described as the Gaussian distribution (standard deviation σ) of a dihedral angle (Brüshweiler and Case, 1994) is considered. This model is characterized by three parameters, P, Φ_m, and σ. The last model (**C**) is based on the two-site jump motion between the N- and S-type sugar conformations (e.g., Rinkel and Altona, 1987). Principally the two-site jump model needs the five parameters, P_N, Φ_{mN}, P_S, Φ_{mS}, and %S; P and Φ_m being for the N- and S-type sugars and the percent fraction of S-type sugar, respectively. Since the number of observed J values was three, two parameters, P_N and Φ_{mN}, were determined empirically and kept during the calculation, i.e., $P_N = 22°$ and $\Phi_{mN} = 36.4°$,

which were the mean values for the 14 published X-ray structures of N-type deoxyribose (van Wijk et al., 1992). With our treatment, models (**A**), (**B**), and (**C**) had two (P, Φ_m), three (P, Φ_m, σ), and three (P_S, Φ_{mS}, %S) adjustable parameters, respectively.

The Gaussian distribution of a dihedral angle model (Brüshweiler and Case, 1994) has been applied to the generalized Karplus equation (Kojima et al., 1998a), but not yet for conformational analysis of the DNA sugar ring. The conformational averaging effects of cos(nθ) and sin(nθ) were analytically expressed for $\sigma \ll \pi$ as $\exp(-n^2\sigma^2/2)*\cos(n\theta)$ and $\exp(-n^2\sigma^2/2)*\sin(n\theta)$, respectively, where θ and σ are the center and standard deviation of the Gaussian distribution, and n is a natural number. In Table 3 the generalized Karplus equations for β-D-deoxyribose (Haasnoot et al., 1980; Wijmenga et al., 1993) characterized by the Gaussian distribution model are shown. Here Φ_{HH}, Φ_m, P, and σ are the dihedral angle, the pucker amplitude, the phase angle of pseudorotation, and the standard deviation of the dihedral angle Φ_{HH}, respectively. The unit for σ is radian, while the others (Φ_{HH}, Φ_m, P) are in degrees. ΔJ is a correction term for the Barfield transmission effect (Barfield, 1980; de Leeuw et al., 1983). Since the ΔJ term is not treated as a deviation of the dihedral angles in our Gaussian distribution model, these equations may have small systematic errors in the range of $144° < P < 324°$ for $J_{H1'H2''}$ and $198° < P < 378°$ for $J_{H2'H3'}$ if $\sigma \neq 0$.

Using the Karplus equations listed in Table 3 the adjustable parameters of each motional model were optimized by minimizing the RMSD of the observed and simulated J-coupling constants. Three J-coupling constants, $J_{H1'H2'}$, $J_{H1'H2''}$ and $J_{H1'H2'}+J_{H2'H3'}$, were used for the optimization. The resulting parameters are shown in Table 4. The bold values were judged to be acceptable based on the criteria used in Table 2. As described above, the single conformation model, model (**A**), was not acceptable. However, assuming the fluctuation of the sugar dihedral angles about 27° (model **B**) or the equilibrium between the N- and S-type sugar conformations with the 68% S-type fraction (model **C**), the observed proton-proton vicinal J-coupling constants were well explained. Empirically, the sugar pucker amplitude Φ_m has been found between 26° and 44° in 65 published X-ray structures of deoxyriboses (van Wijk et al., 1992), thus $\Phi_m = 21°$ in model (**B**) is unacceptably low. The fluctuation angle $\sigma = 27°$ in model (**B**) is quite large judged from its basic assumption $\sigma \ll \pi$. On the contrary, all parameters in model (**C**) appear to be reasonably acceptable. As a result, model (**C**) is more probable than model (**B**).

Discussion

Stereoselective deuterium labeling

Deuterium labeling has been used in NMR studies on proteins and nucleic acids for more than 30 years, and now it is an essential technique for the analysis of larger molecules (e.g. Kay and Gardner, 1997; Gardner and Kay, 1998; and references therein). In most cases 50–90% uniform labeling is employed instead of stereoselective labeling because the former is easier than the latter in sample preparation. Both procedures can suppress the proton-proton dipolar interaction and the dipolar interference in J-coupling (Harbison, 1993; Zhu et al., 1994; Cavanagh et al., 1996) by diluting the proton density. The apparent line widths will be different because of the differences in the J-coupling constants and the isotope shifts with the two methods. Uniform deuterium labeling produces an ensemble of the isotopomers but stereo-selective deuterium labeling yields only one isotopomer, that is, a uniformly labeled sample has an ensemble of J-coupling constants and chemical shifts. The resulting apparent line width of a uniformly labeled sample is larger than that of a stereoselectively labeled sample (Kushlan and LeMaster, 1993). The COSY spectrum of a uniformly labeled sample will not be much different from that of a non-labeled sample, as there are identical numbers of cross peaks with a complicated splitting pattern. Theoretical NOE analysis of a uniformly labeled sample is quite difficult (Zolnai et al., 1998) due to the presence of the isotopomer ensemble. Thus, in general, information obtained from a stereoselectively deuterium-labeled sample is more quantitative than that from a uniformly labeled sample.

Stereoselective deuterium labeling at the 2′ position has several advantages. The most important one is the simple and precise determination of the J-coupling constants, as shown in this report. This is mainly due to the elimination of the large J-coupling constants ($\sim$ 14 Hz) and the strong dipolar interaction (1.75 Å) between the methylene protons. The absence of the geminal J-coupling constant leads not only to simplification of the spin system but also to elimination of the ambiguity hidden in the geminal J-coupling constant value itself. The J-coupling constant between the geminal protons of a methylene group ($\sim$ 14 Hz) has been supposed to be constant and not

Table 3. Generalized Karplus equations for β-D-deoxyribose with the Gaussian distribution model[a]

$$
\begin{aligned}
{}^3J_{H1'H2'} &= 5.6920 + (-0.99)\exp(-\sigma^2/2)\cos\Phi_{H1'H2'} + 4.2782\exp(-2\sigma^2)\cos 2\Phi_{H1'H2'} + (-0.8084)\exp(-2\sigma^2)\sin 2\Phi_{H1'H2'} \\
{}^3J_{H1'H2''} &= 5.6920 + (-0.99)\exp(-\sigma^2/2)\cos\Phi_{H1'H2''} + 4.2782\exp(-2\sigma^2)\cos 2\Phi_{H1'H2''} + (-0.5385)\exp(-2\sigma^2)\sin 2\Phi_{H1'H2''} + \Delta J \\
{}^3J_{H2'H3'} &= 5.8540 + (-0.99)\exp(-\sigma^2/2)\cos\Phi_{H2'H3'} + 4.6736\exp(-2\sigma^2)\cos 2\Phi_{H2'H3'} + (+1.2555)\exp(-2\sigma^2)\sin 2\Phi_{H2'H3'} + \Delta J \\
{}^3J_{H2''H3'} &= 5.8540 + (-0.99)\exp(-\sigma^2/2)\cos\Phi_{H2''H3'} + 4.6736\exp(-2\sigma^2)\cos 2\Phi_{H2''H3'} + (+0.9856)\exp(-2\sigma^2)\sin 2\Phi_{H2''H3'} \\
{}^3J_{H3'H4'} &= 4.5879 + (-0.91)\exp(-\sigma^2/2)\cos\Phi_{H3'H4'} + 3.6905\exp(-2\sigma^2)\cos 2\Phi_{H3'H4'} + (-0.0670)\exp(-2\sigma^2)\sin 2\Phi_{H3'H4'}
\end{aligned}
$$

$$
\begin{aligned}
\Phi_{H1'H2'} &= 121.4 + 1.03\,\Phi_m\cos(P - 144) \\
\Phi_{H1'H2''} &= 0.9 + 1.02\,\Phi_m\cos(P - 144) \\
\Phi_{H2'H3'} &= 2.4 + 1.06\,\Phi_m\cos(P) \\
\Phi_{H2''H3'} &= 122.9 + 1.06\,\Phi_m\cos(P) \\
\Phi_{H3'H4'} &= -124.0 + 1.09\,\Phi_m\cos(P + 144)
\end{aligned}
$$

$$
\Delta J = \begin{cases} -2.0\cos^2(P - 234) & \text{for } 144^\circ < P < 324^\circ \text{ for } J_{H1'H2''} \\ -0.5\cos^2(P - 288) & \text{for } 0^\circ \le P < 18^\circ \text{ and } 198^\circ < P \le 360^\circ \text{ for } J_{H2'H3'} \end{cases}
$$

[a]Generalized Karplus parameters (Haasnoot et al., 1980; Wijmenga et al., 1993) localized for β-D-deoxyribose with the classical harmonic motion described as a Gaussian distribution (Brüshweiler and Case, 1994). σ is the standard deviation of the dihedral angle (in rad). Φ_{HH}, Φ_m and P are the dihedral angle, pucker amplitude, and phase angle of pseudorotation, respectively (in deg). ΔJ is a correction term for the Barfield transmission effect (Barfield, 1980; de Leeuw et al., 1983). If $\sigma = 0$, these equations are identical to the original generalized Karplus equation (Haasnoot et al., 1980; Wijmenga et al., 1993).

to change with the DNA conformation. Actually this assumption is reasonable assuming a systematic error of 1–2 Hz. The experimental determination of this geminal J-coupling constant is difficult because of the overlapping of the 2′ and/or 2″ proton resonances and the strong coupling conditions. The absence of a dipolar interaction between the methylene protons causes significant lengthening of the relaxation time (sharpening of the signals) and attenuation of the dipolar interference of the J-coupling constant. The dipolar interference makes the apparent J-coupling constants small. Stereoselective deuterium labeling is necessary to increase the precision and accuracy of the observed J-coupling constants.

Although deuterium-labeling has many advantages, as described above, it causes some systematic errors. They are the J-coupling constants between a proton and a deuteron, and the dipolar and scalar relaxation due to the proton-deuteron interaction. First, the proton-deuteron J-coupling constants are expected to be about 15% of the proton-proton ones, where 15% is the relative ratio of the gyro-magnetic ratio of deuterons to protons (γ_{2H}/γ_{1H}). The J-coupling constant between the proton and deuteron at a geminal position ($^2J_{1H2H}$) is expected to be about 2 Hz based on that for protons ($^2J_{1H1H}$), 14 Hz. In general the vicinal J-coupling constants ($^3J_{1H2H}$) are smaller than the geminal ones ($^2J_{1H2H}$), and the magnitude of $^3J_{1H2H}$ is 1 Hz or less. Since the nuclear spin of deuteron is 1, the proton resonance becomes a triplet due to proton-deuteron J-coupling. The proton-deuteron J-coupling constant clearly affects the apparent proton-proton J-coupling constants. Since the proton-deuteron J-coupling constants are smaller than the line width of the DNA oligomer employed in the present work, only proton line broadening is observed as an apparent contribution of the proton-deuteron J-coupling constants. This error can be eliminated by deuterium decoupling and/or the occurrence of scalar relaxation of the second kind. Second, the deuteron will not be negligible in the proton relaxation process a priori, and in our system the determined T_1 and T_2^* values may have some systematic errors originating from the deuterium. The relative magnitude of the proton-deuteron dipolar interaction was roughly determined to be less than 2% of that of the proton-proton one based on the $(\gamma_{2H}/\gamma_{1H})^2$ value. The scalar relaxation of the second kind has a small contribution to proton T_2, 1–2%, calculated assuming the deuterium T_1 value is 1 ms. Considering these systematic errors introduced by deuterium labeling, the resulting phenomenon is line broadening of the proton resonance and a systematic decrease in the apparent proton-proton J-coupling constants for the in-phase spectrum. These systematic errors were not eliminated, although they are very small and comparable to experimental errors.

J-coupling constant determination

Direct reading of the J-splitting from the COSY spectrum causes a systematic increase in the apparent J-coupling constants because of the cancellation of the positive and negative peaks (Neuhaus et al.,

Table 4. Single conformation model and two motional models, and simulated J coupling constants for the 3′ terminal C10 residue of the 2″- or 2′-deuterium-labeled DNA decamer[a]

(A) Single conformation model							
$J_{H1'H2'}$	$J_{H1'H2'} + J_{H2'H3'}$	$J_{H1'H2''}$	$J_{H1'H2''} + J_{H2''H3'}$	P (deg)	Φ_m (deg)		RMSD
7.9	17.3	7.8	10.7	100.9	23.9		0.7
(B) Single conformation with Gaussian distribution model							
$J_{H1'H2'}$	$J_{H1'H2'} + J_{H2'H3'}$	$J_{H1'H2''}$	$J_{H1'H2''} + J_{H2''H3'}$	P (deg)	Φ_m (deg)	σ (deg)	RMSD
7.3	15.1	6.9	10.7	**108.0**	**21.2**	**26.6**	**0.0**
(C) N-S two-site jump model							
$J_{H1'H2'}$	$J_{H1'H2'} + J_{H2'H3'}$	$J_{H1'H2''}$	$J_{H1'H2''} + J_{H2''H3'}$	P_S (deg)	Φ_{mS} (deg)	%S	RMSD
7.3	13.9	6.9	10.7	**163.4**	**31.7**	**67.8**	0.0

[a]J values in Hz.

(**A**) Single sugar conformation model characterized by the two parameters of the phase angle of pseudorotation, P, and the pucker amplitude, Φ_m, where each parameter was optimized by minimizing the RMSD between observed and simulated J coupling constants. The generalized Karplus equations used for all calculations are listed in Table 3. The bold values were judged to be acceptable. (**B**) Classical harmonic motion (Brüshweiler and Case, 1994) described as the Gaussian distribution (standard deviation σ) of a dihedral angle. P, Φ_m and σ were optimized. (**C**) Two-site jump model between the N- and S-type sugar conformations. The N-type conformation is fixed as P = 22° and $\Phi_m = 36.4°$, which are the mean values for the 14 published X-ray structures of N-type deoxyribose (van Wijk et al., 1992). P_S, Φ_{mS}, and %S are optimized.

1985). Thus we have performed line fitting of the 1D spectrum, although the 2D COSY spectrum has a lot of advantages; for example, the peaks are well separated and the number of determinable J values increases. Very recently a band-selective COSY experiment combined with stereospecific deuterium labeling at the 2′ position was applied to determine the J coupling constants of a DNA dodecamer (Yang et al., 1997), where our deuterium-labeling procedure (Kawashima et al., 1995b) was used to prepare a 2′-R deuterium-labeled DNA oligomer. Spectral simulations such as SPHINX and LINSHA may counteract the cancellation effect on the 2D COSY spectrum. If a band-selective COSY experiment is used for a stereospecific deuterium-labeled sample in combination with a simulation procedure such as SPHINX and LINSHA, the precision of the determined J values could be comparable to that with our 1D procedure, 0.1–0.2 Hz. Potentially their 2D method is useful for studying the J coupling constants of a larger complex system.

Fluctuation contribution to the Karplus parameters and the sugar conformation

The generalized Karplus parameters used in this report (Haasnoot et al., 1980; Wijmenga et al., 1993) may have systematic errors due to conformational averaging and thermal fluctuation. The effect of conformational averaging was avoided since the Karplus parameters given by Haasnoot et al. (1980) were derived from conformationally rigid molecules, largely 6-membered rings with holding groups. On the other hand, the contribution from thermal fluctuation through fast time scale motions below 1 ns was not negligible, as reported previously (Hoch et al., 1985; Brüschweiler and Case, 1994). By adding the harmonic motion to the Karplus relation as the Gaussian distribution of dihedral angles (model **B** in our case), the contribution of thermal fluctuation could be overestimated. However, the thermal fluctuation contribution to the Karplus parameters was assumed to be minimized and, in fact, small, since quite rigid molecules were used and the error of the Karplus parameters was less than 0.48 Hz (Haasnoot et al., 1980).

For the 3′ terminal residue the order parameter S^2 of the 3′CH site was determined to be 0.5 and thus smaller than that of the other sites ($S^2 = 0.8 \pm 0.1$) from the results of a ^{13}C relaxation study of a DNA decamer (Kojima et al., 1998b). These differences are reasonably explained by the increase in the sugar flexibility induced by the lack of the 3′ phosphate group. On the other hand, the 5′ terminal residue does not have a phosphate group either. In fact, both a ^{13}C relaxation study (Kojima et al., 1998b) and a proton-proton J-coupling constants study (e.g. Weisz et al., 1992) showed a small difference for the 5′ terminal residue, which was explained by the increase in the sugar flexibility. However, the difference found in the 3′ terminal residue is much larger than that in the 5′ one, and the 5′ methylene group would be more im-

portant than the sugar ring for canceling the impact of the lack of a phosphate group.

Simulation of J-coupling constants

For the C10 residue both the Gaussian distribution model (**B**) and the two-site jump model (**C**) could explain the observed J-coupling values. To make matters worse, it is highly likely that another motional model can explain them. However, based on many experimental data and numerical approaches, the N-S two-site jump model is more probable (Lane, 1993; Schmitz et al., 1993; Ulyanov et al., 1995; Tonelli and James, 1998). In our results an unacceptably lower pucker amplitude, $\Phi_m = 21°$, and a quite large fluctuation, $\sigma = 27°$, in model (**B**) indicate that model (**B**) is less probable than model (**C**) (vide supra). So far the intrinsic differences between the two-site jump model and the single conformation models with and without the Gaussian distribution of the dihedral angles are not clear from the viewpoint of the J-coupling constants. Here this is evaluated by a simple simulation as follows.

The proton-proton vicinal J coupling constants ($^3J_{H1'H2'}$, $^3J_{H1'H2''}$, $^3J_{H2'H3'}$, $^3J_{H2''H3'}$, $^3J_{H3'H4'}$) can be related to the DNA sugar-ring conformation using the generalized Karplus equations (Haasnoot et al., 1980; Wijmenga et al., 1993) (see Table 3). Each dihedral angle Φ_{HH} of the DNA sugar ring was calculated from pseudorotation angle P and pucker amplitude Φ_m. The 1000 data sets of these five ^3J coupling constants were systematically computed based on the two-site jump model between the N- and S-type sugar conformations. Five parameters were randomly generated for each data set, two pseudorotation angles of the N-form (P_N) and S-form (P_S), two pucker amplitudes of the N-form (Φ_{mN}) and S-form (Φ_{mS}), and the percentage of the S-form fraction (%S). The %S values were uniformly randomized in the range of 0 to 100. The other parameters were randomized to form the Gaussian distribution, where the distribution center and standard deviation were 22.0° and 8.0° for P_N, 162° and 15° for P_S, and 36.4° and 3.0° for both Φ_{mN} and Φ_{mS}, respectively. All of these values were obtained empirically based on the 14 and 51 published X-ray structures of N- and S-type deoxyriboses, respectively (see van Wijk et al., 1992). For example, Φ_{mS} ranged from 26° to 44°, with an average of 36.4°, in the crystal structure, and the standard deviation was estimated by dividing the maximum limit by 2.5 (assuming a 99% confidence level). The other parameters were obtained by a similar method. The two-site jump model used for these simulations (designated as model **C**′) was different from that used for the sugar conformational analysis shown in Table 3 (model **C**), that is, the number of variable parameters was five for the simulation (model **C**′) but only three for the experimental data analysis (model **C**).

These 1000 data sets generated with the two-site jump model (model **C**′) were subjected to fitting with the single conformation models (models **A** and **B**). The results are shown in Figure 2, where P, Φ_m, σ, RMSD, and %S are identical to those defined in Tables 2 and 4 (vide supra). The fitted results for the single conformation models with (model **B**) and without (model **A**) the Gaussian distribution of the dihedral angles are shown on the left and right sides of Figure 2, respectively. Three or four parameters, P, Φ_m, RMSD, and/or σ, were plotted against the %S values, the individual circle in each plot corresponding to the one data set containing five J-coupling constants. Although the two-site jump model used was the five-parameter model and the single conformation models were the two- and three-parameter models, all 1000 data sets converged for model **B** (three-parameter) and 942 out of the 1000 for model **A** (two-parameter). Since 58 out of the 1000 data sets dit not converge for model **A**, the difference in the number of adjustable parameters, i.e. two for model **A** and three for model **B**, may play an important role in the convergence. The RMSD values for model **A** ranged up to 1.8 Hz, and those for model **B** were less than 0.5 Hz.

Considering experimental and intrinsic Karplus parameter errors, 0.1–0.2 Hz + 0.48 Hz $\approx$ 0.7 Hz, simple RMSD analysis of J-coupling constants cannot distinguish the two-site jump model (model **C**′, five-parameter) from the single conformation model with the Gaussian distribution of the dihedral angles (model **B**, three-parameter). When the %S values are less than 15% or more than 90%, the RMS difference of the J-values between model **C**′ (two-site jump model) and model **A** (single conformation model) is less than 0.7 Hz. Thus the J-coupling constants generated with the two-site jump model (models **C** and **C**′) are reproducible using the single conformation model (**A**) in these limited %S value ranges.

The structural parameters in Figure 2 have some remarkable features. All the optimized parameters show a transition at %S $\sim$ 55, that is, the minimum values were found for Φ_m, the maximum ones for σ and RMSD, and intermediate ones for P. On comparison of the left and right sides in Figure 2, a similar dependence on %S was found for each corresponding

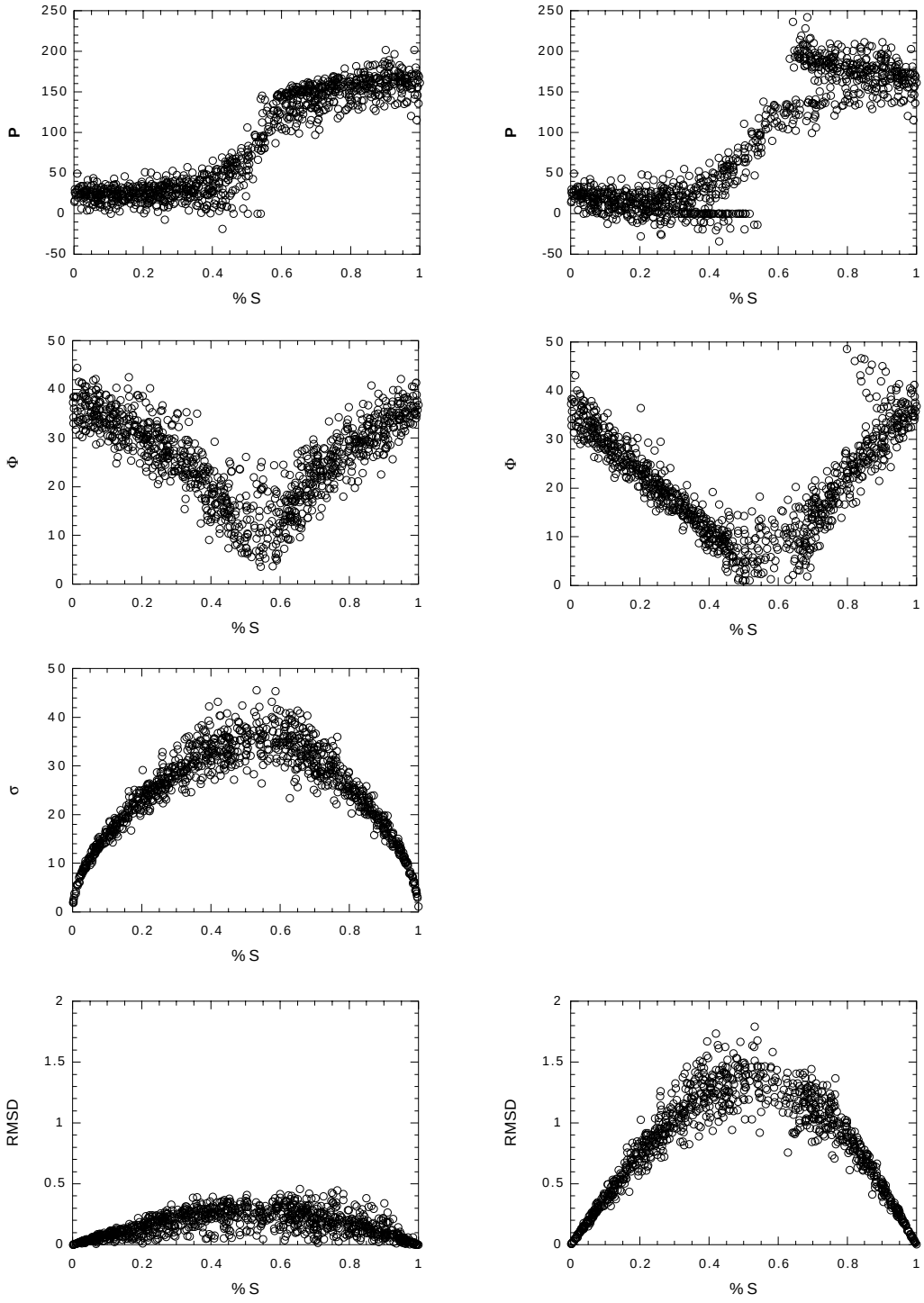

Figure 2. The relationship between the fraction of the S-conformer (%S) in the NS two-site jump model and the other parameters in the single conformation model with (left) and without (right) the Gaussian distribution of the dihedral angle. The pseudorotation angle (P, in degrees), the puckering amplitude (Φ, in degrees), the Gaussian distribution angle (σ, in degrees), and the root mean square deviation (RMSD, in Hz), from top to bottom, were obtained through a process in which five J coupling constants for the deoxyribose ring were generated based on the two-site jump model and then subjected to fitting with the single conformation models.

parameter. Many Φ_m values in Figure 2 are unacceptably small on the basis of the 51 X-ray structures, where Φ_m are in the range of 26° to 44°, in the ranges of $15 < \%S < 90$ (model **A**) and $25 < \%S < 80$ (model **B**). Many σ values are larger than those assumed with the Gaussian distribution model, where $\sigma \ll \pi$ (vide supra). Thus, from the viewpoint of physical parameters such as Φ_m and σ, the single conformation models are clearly different from the two-site jump model, especially in the range 25 to 80 of %S.

In Figure 3 three histograms of the pseudorotation angle P are shown, which were obtained with the five-parameter two-site jump model (model **C**′, top), three-parameter single conformation model (model **B**, middle), and two-parameter single conformation model (model **A**, bottom). In the top histogram the generated N- and S-type conformations are shown, and in the other two the resulting conformations are presented. The three histograms are not very different from each other, the top and middle ones especially being quite similar. It demonstrates the difficulty in distinguishing them. Compared to the top one, the middle and bottom ones exhibit a slightly different tendency. First, the standard deviation of the pseudorotation angle P for each N- and S-type conformation is small in the middle one but large in the bottom one. Second, the distribution center of each S-type conformation of the bottom one is larger than in the others, and this seems to be unrealistic judging from the empirical values of the pseudorotation angle P. These small differences can be used to distinguish each other, but not very useful.

From these simulations, we point out that simple RMSD analysis of J-coupling constants cannot distinguish the two-site jump model from the single conformation with Gaussian fluctuation model, even when the five proton-proton J-coupling constants can be determined accurately and precisely. If %S values are less than 15 or more than 90, it is completely meaningless to distinguish them. On the contrary, if we carefully analyze J-coupling constants with empirical knowledge of the Φ_m and σ values, it is clearly possible to distinguish the two-site jump model from the single conformation with Gaussian fluctuation model, especially in the range of 25 to 80 of %S.

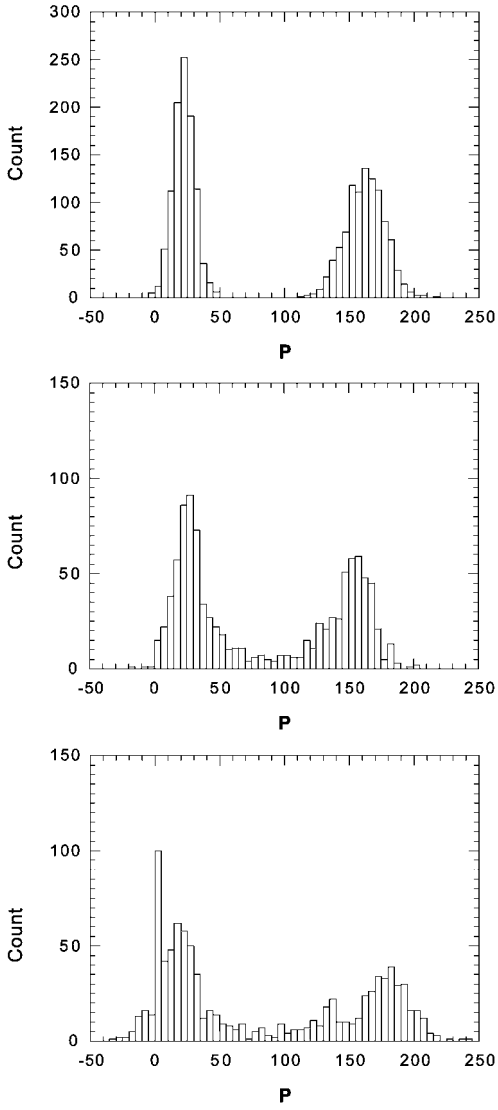

Figure 3. Histograms of the pseudorotation angle, generated with the NS two-site jump model (top), and fitted with the single conformation model with (middle) and without (bottom) the Gaussian distribution of the dihedral angle. For the two-site jump model the N- and S-type conformations were generated assuming the pseudorotation angles 22° ± 8° and 162° ± 15°, and the pucker amplitude 36.4° ± 3°, as the normal distribution center and standard deviation, respectively.

Acknowledgements

We wish to thank Dr. Nikolai B. Ulyanov (UCSF) for the helpful discussion. This work was supported by a Grant-in-Aid for Basic Scientific Research, Category B (No. 09480176), from the Ministry of Education, Science and Culture, Japan, grant RG401/95 from the Human Frontier Science Program (Strasbourg, France), and a grant from CREST (Core Research Evolutional Science and Technology) of the Japan Science and Technology Corporation (JST).

References

Abragam, A. (1961) *Principles of Nuclear Magnetism*, Chapter VIII, Equations 76, 79, and 104, Oxford University Press, Oxford.

Agback, P., Maltseva, T.V., Yamakage, S.-I., Nilson, F.P.R., Földesi, A. and Chattopadhyaya, J. (1994) *Nucleic Acids Res.*, **22**, 1404–1412.

Barfield, M. (1980) *J. Am. Chem. Soc.*, **102**, 1–7.

Bax, A. and Lerner, L. (1988) *J. Magn. Reson.*, **79**, 429–438.

Brüschweiler, R. and Case, D.A. (1994) *J. Am. Chem. Soc.*, **116**, 11199–11200.

Cavanagh, J., Fairbrother, W.J., Palmer III, A.G. and Skelton, N.J. (1996) *Protein NMR Spectroscopy: Principle and Practice*, Academic Press, London.

Chazin, W.J., Wüthrich, K., Hyberts, S., Rance, M., Denny, W.A. and Leupin, W. (1986) *J. Mol. Biol.*, **190**, 439–453.

Conte, M.R., Bauer, C.J. and Lane, A.N. (1996) *J. Biomol. NMR*, **7**, 190–206.

Curley Jr., W., Panigot, M.J., Hansen, A.P. and Fesik, S.W. (1994) *J. Biomol. NMR*, **4**, 335–340.

de Leeuw, F.A.A.M., van Beuzekom, A. and Altona, C. (1983) *J. Comput. Chem.*, **4**, 438–448.

Eimer, W., Williamson, J.R., Boxer, S.G. and Pecora, R. (1990) *Biochemistry*, **29**, 799–811.

Foldesi, A., Nilson, F.P., Glemarec, C., Gioeli, C. and Chattopadhyaya, J. (1993) *J. Biochem. Biophys. Methods*, **26**, 1–26.

Gardner, K.H. and Kay, L.E. (1998) *Annu. Rev. Biophys. Biomol. Struct.*, **27**, 357–406.

Haasnoot, C.A.G., de Leeuw, F.A.A.M. and Altona, C. (1980) *Tetrahedron*, **36**, 2783–2792.

Harbison, G.S. (1993) *J. Am. Chem. Soc.*, **115**, 3026–3027.

Hoch, J.C., Dobson, C.M. and Karplus, M. (1985) *Biochemistry*, **24**, 3831–3841.

Huang, W.C., Orban, J., Kintanar, A., Reid, B.R. and Drobny, G.P. (1990) *J. Am. Chem. Soc.*, **112**, 9059–9068.

Kawashima, E., Aoyama, Y., Sekine, T., Nakamura, E., Kainosho, M., Kyogoku, Y. and Ishido, Y. (1993) *Tetrahedron Lett.*, **34**, 1317–1320.

Kawashima, E., Aoyama, Y., Radwan, M.F., Miyahara, M., Sekine, T., Kainosho, M., Kyogoku, Y. and Ishido, Y. (1995a) *Nucleotides Nucleosides*, **14**, 333–336.

Kawashima, E., Aoyama, Y., Sekine, T., Miyahara, M., Radwan, M.F., Nakamura, E., Kainosho, M., Kyogoku, Y. and Ishido, Y. (1995b) *J. Org. Chem.*, **60**, 6980–6986.

Kay, L.E. and Gardner, K.H. (1997) *Curr. Opin. Struct. Biol.*, **7**, 722–731.

Keepers, J.W. and James, T.L. (1984) *J. Magn. Reson.*, **57**, 404–426.

Kojima, C., Kawashima, E., Toyama, K., Ohshima, K., Sekine, T., Ishido, Y., Kainosho, M. and Kyogoku, Y. (1998a) *J. Biomol. NMR*, **11**, 103–109.

Kojima, C., Ono, A., Kainosho, M. and James, T.L. (1998b) *J. Magn. Reson.*, **135**, 310–333.

Kushlan, D.M. and LeMaster, D.M. (1993) *J. Biomol. NMR*, **3**, 701–708.

Kyogoku, Y., Kojima, C., Lee, S.J., Tochio, H., Suzuki, N., Matsuo, H. and Shirakawa, M. (1995) *Methods Enzymol.*, **261**, 524–541.

Lane, A.N. (1993) *Prog. NMR Spectrosc.*, **25**, 481–505.

Marion, D., Ikura, M., Tschudin, R. and Bax, A. (1989) *J. Magn. Reson.*, **85**, 393–399.

Neuhaus, D., Wagner, G., Vasak, M., Kagi, J.H. and Wüthrich, K. (1985) *Eur. J. Biochem.*, **151**, 257–273.

Ono, A., Tate, S., Ishido, Y. and Kainosho, M. (1994) *J. Biomol. NMR*, **4**, 581–586.

Rinkel, L.J. and Altona, C. (1987) *J. Biomol. Struct. Dyn.*, **4**, 621–649.

Salazar, M., Champoux, J.J. and Reid, B.R. (1993) *Biochemistry*, **32**, 739–744.

Schmitz, U., Ulyanov, N.B., Kumar, A. and James, T.L. (1993) *J. Mol. Biol.*, **234**, 373–389.

Schmitz, U. and James, T.L. (1995) *Methods Enzymol.*, **261**, 3–44.

Tonelli, M. and James, T.L. (1998) *Biochemistry*, **37**, 11478–11487.

Ulyanov, N.B., Schmitz, U., Kumar, A. and James, T.L. (1995) *Biophys. J.*, **68**, 13–24.

van Wijk, J., Huckriede, B.D., Ippel, J.H. and Altona, C. (1992) *Methods Enzymol.*, **211**, 286–306.

Wang, A.C., Kim, S.-G., Flynn, P.F., Chou, S.-H., Orban, J. and Reid, B.R. (1992) *Biochemistry*, **31**, 3940–3946.

Weisz, K., Shafer, R.H., Egan, W. and James, T.L. (1992) *Biochemistry*, **31**, 7477–7487.

Widmer, H. and Wüthrich, K. (1986) *J. Magn. Reson.*, **70**, 270–279.

Widmer, H. and Wüthrich, K. (1987) *J. Magn. Reson.*, **74**, 316–336.

Wijmenga, S.S., Mooren, M.M.W. and Hilbers, C.W. (1993) In *NMR in Macromolecules* (Ed., Roberts, G.C.), IRL Press, Oxford, pp. 217–288.

Yamakage, S.-I., Maltseva, T.V., Nilson, F.P., Földesi, A. and Chattopadhyaya, J. (1993) *Nucleic Acids Res.*, **21**, 5005–5011.

Yang, J., Silks, L., Wu, R., Isern, N., Unkefer, C. and Kennedy, M.A. (1997) *J. Magn. Reson.*, **129**, 212–218.

Zhu, L.M., Reid, B.R., Kennedy, M.A. and Drobny, G.P. (1994) *J. Magn. Reson.*, **A111**, 195–202.

Zolnai, Z., Juranitc, N. and Macura, S. (1998) *J. Biomol. NMR*, **12**, 333–337.